

A Class of Electron-Transporting Vinyllogous Tetrathiafulvalenes Constructed by the Dimerization of Core-Expanded Naphthalenediimides

Yunbin Hu,[†] Zhongli Wang,[†] Xu Zhang,[‡] Xiaodi Yang,[‡] Congwu Ge,[†] Lina Fu,^{†,§} and Xike Gao^{*,†,§}

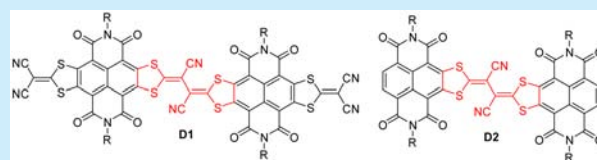
[†]Key Laboratory of Synthetic and Self-Assembly Chemistry for Organic Functional Molecules, Shanghai Institute of Organic Chemistry, Chinese Academy of Sciences, 345 Lingling Road, 200032 Shanghai, China

[‡]Laboratory of Advanced Materials, Fudan University, Shanghai 200433, China

[§]School of Materials Science and Engineering, East China University of Science and Technology, Shanghai 200237, China

S Supporting Information

ABSTRACT: The combination of the (1,3-dithiol-2-ylidene)malononitrile (DTYM) and/or (1,3-dithiol-2-ylidene)acetonitrile (DTYA) moieties with naphthalenediimide (NDI) core affords two singly linked NDI-based dimers, (DTYM-NDI-DTYA)₂ (**D1**) and (NDI-DTYA)₂ (**D2**), which both contain a dicyano-substituted vinyllogous tetrathiafulvalene (TTF) unit. The synthesis, thermal/optical/electrochemical properties of **D1** and **D2**, and their primary applications in n-channel organic thin film transistors are studied. The results demonstrate that these NDI-fused vinyllogous TTFs are excellent electron acceptors, and their further applications are promising.



First reported by Yoshida and co-workers in 1983,¹ vinyllogous tetrathiafulvalenes (TTFs) are a class of TTF analogues with one vinyl spacer between the two 1,3-dithiole rings (Figure 1) and usually exhibit stronger electron-donating

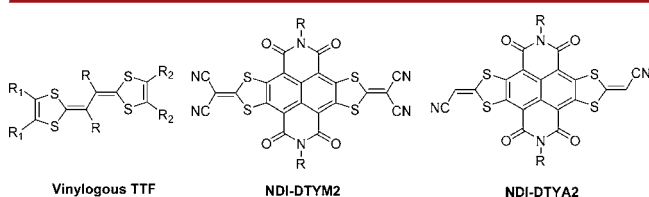


Figure 1. Chemical structures of vinyllogous TTF and two core-expanded naphthalenediimides NDI-DTYM2 and NDI-DTYA2.

properties and smaller on-site Coulombic repulsion than the corresponding TTFs. These features make vinyllogous TTFs suitable for constructing organic conductors and superconductors. One superconducting salt containing a donor with a vinyllogous TTF framework was reported in 1995.² Similar to the common TTFs, the molecular backbones of the unsubstituted vinyllogous TTFs ($R = H$) are generally planar,^{2,3} but the addition of bulky substituents ($R = \text{alkyl, aryl, etc.}$) on the vinyl position of vinyllogous TTFs usually leads to the nonplanar molecular backbones, and this barely modifies the molecular donor ability.⁴ In 2005, the electron-withdrawing cyano groups were introduced at the vinyl position, and the resulting vinyllogous TTFs ($R = CN$) showed much higher oxidation potentials than the unsubstituted analogues ($R = H$) with half-wave potentials ≥ 0.95 V (vs Ag/AgCl),⁵ indicating that these vinyllogous TTFs are the weak electron donors. One question is whether we can

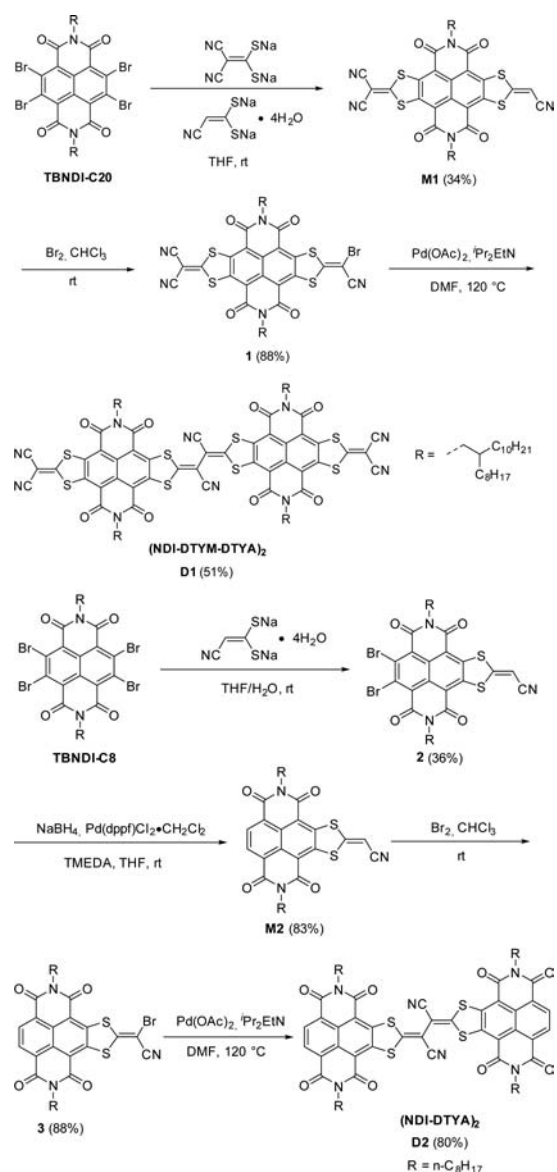
create a class of highly soluble electron-transporting vinyllogous TTFs that have twisted molecular backbones and can act as electron acceptors rather than the donors. On the other hand, vinyllogous TTFs have been successfully used as versatile building blocks for constructing new organic functional materials.⁶ Therefore, vinyllogous TTFs should be endowed with new chemistry and new functions for their next applications.

In recent years, we have developed a series of core-expanded naphthalenediimides (NDIs) for organic electronic devices.⁷ Among them, NDI-DTYM2 and NDI-DTYA2 (Figure 1) are the most representative building blocks, bearing two (1,3-dithiol-2-ylidene)malononitrile (DTYM)^{7a-d} and two (1,3-dithiol-2-ylidene)acetonitrile (DTYA)^{7f} moieties, respectively. It should be noted that the DTYA moiety allows further π -extension by chemical modification at the vacant vinyl position.^{7f} In this contribution, we combine DTYM and/or DTYA moieties with the NDI core, affording two singly linked NDI-based dimers, (DTYM-NDI-DTYA)₂ (**D1**) and (NDI-DTYA)₂ (**D2**) (Scheme 1), which both contain a dicyano-substituted vinyllogous TTF unit. Therefore, **D1** and **D2** can be viewed as a class of vinyllogous TTFs with the fused NDI moieties. We describe here the synthesis and thermal/optical/electrochemical properties of **D1** and **D2** and their primary applications in n-channel organic thin film transistors. The results demonstrate that these NDI-fused vinyllogous TTFs (**D1** and **D2**) are electron acceptors that transport electrons efficiently.

As depicted in Scheme 1, the synthesis of **D1** and **D2** started from the corresponding 2,3,6,7-tetrabromonaphthalenediimides

Received: December 4, 2016

Published: January 11, 2017

Scheme 1. Synthesis of NDI-Fused Vinyllogous TTFs (**D1** and **D2**)

(TBNDIs) that were readily prepared by the reported procedures.⁸ TBNDI-C20 was used to react with the sodium salts of 1,1-dicyanoethylene-2,2-dithiolate and 1-cyanoethylene-2,2-dithiolate by a one-pot nucleophilic aromatic substitution (S_NAr) reaction, affording the key intermediate **M1** in 34% yield. The S_NAr reaction of TBNDI-C8 with 1 equiv of sodium 1-cyanoethylene-2,2-dithiolate gave a dibromo-NDI-DTYA derivative (**2**, 36% yield) that was readily converted to intermediate **M2** in 83% yield through the $NaBH_4$ -involved reduction. The treatment of **M1** and **M2** with bromine conveniently afforded the corresponding bromides **1** and **3** with almost the same yield of 88%. Several synthetic methods were attempted for the synthesis of **D1** but failed, including the straightforward oxidative coupling reaction of **M1** and hexabutyl distannane-mediated homocoupling reaction of bromide **1**, according to the synthesis of vinyllogous TTFs^{5b} and bis-NDI,⁹ respectively. Finally, **D1** was achieved in 51% yield by the homocoupling reaction of **1** in the presence of $Pd(OAc)_2$ and Pr_2EtN in DMF, according to the modified method of the preparation of 3,3',4,4'-tetracyano-2,2'-

bithiophene.¹⁰ In the same way, **D2** was generated from bromide **3** in an even higher yield of 80%. Compounds **D1** and **D2** both have good solubility in common organic solvents such as dichloromethane, chloroform, toluene, and xylene.

Thermogravimetric analysis (TGA) reveals that the onset decomposition temperatures of **D1** and **D2** are over 370 and 387 °C, respectively (Figure S1). The differential scanning calorimetry (DSC) measurement of **D1** shows no detectable phase transition from room temperature to 300 °C, and that of **D2** displays two weak endothermic (222/266 °C) and exothermic peaks (148/200 °C) before decomposition, implying the solid–solid phase transitions (Figure S2). These results indicate that both **D1** and **D2** have good thermal stability.

Density functional theory (DFT) calculations were performed to investigate the structures and energies of frontier orbitals of compounds **D1** and **D2** (Figure 2, the *N*-groups of **D1** and **D2**

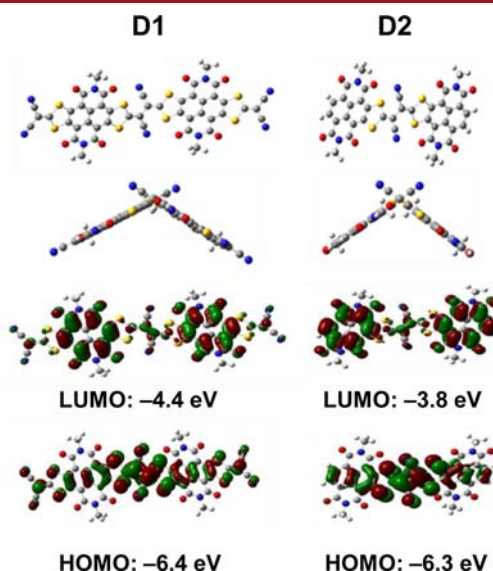


Figure 2. Geometries, frontier orbitals, and MO energies of model molecules for **D1** and **D2** (all of the alkyl chains were replaced by methyl group to simplify the calculations).

were replaced by methyl groups to shorten the calculation time) using the Gaussian 09 program at the B3LYP/6-31G(d,p) level. As shown in Figure 2, the model molecules of **D1** and **D2** both present twisted molecular backbones with intramolecular dihedral angles of 123° and 111°, respectively. The nonplanar molecular backbone structures of **D1** and **D2** endow them with good solubility in organic solvents, which is indicative of their great potentials for solution-processed organic electronic materials. The LUMO orbital wave functions of **D1** and **D2** are mainly localized on the two NDI segments. Their HOMO orbital wave functions are distributed across the whole π -conjugated skeletons except for the imide rings and focus on the vinyllogous TTF unit. The results indicate that there may be considerable intramolecular charge transfer for both **D1** and **D2**. **D1** has much lower LUMO energy (−4.4 eV) than that of **D2** (−3.8 eV) due to the electron-withdrawing feature of DTYM moiety,⁷ while **D1** and **D2** have comparable HOMO energies (−6.4 and −6.3 eV) that may be dominated by the vinyllogous TTF unit. Moreover, we calculated the reorganization energies of model molecules of **D1** and **D2** at DFT level using the B3LYP functional and 6-31G(d,p) basis set. The hole/electron reorganization energies of model molecules of **D1** and **D2** are

507/151 and 739/168 meV, respectively, demonstrating that **D1** and **D2** are easier to transport electrons than holes.¹¹

The absorption spectra of **D1**, **D2**, **M1**, and **M2** in solution and in thin film were recorded to investigate their optical properties (Figure 3 and Figure S3), and the data are collected in Table 1. In

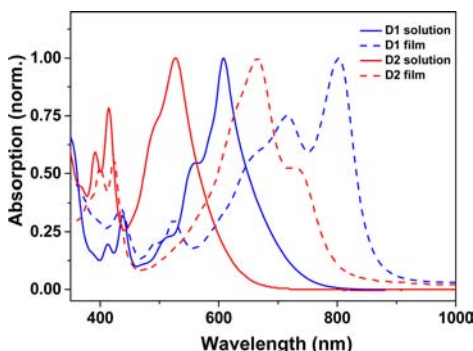


Figure 3. Optical absorption spectra of **D1** and **D2** in CH_2Cl_2 solution and in thin films on quartz substrates.

Table 1. Optical and Electrochemical Properties of **M1**, **M2**, **D1**, and **D2**

	$\lambda_{\text{max}}^{\text{sol}^a}$ (nm)	(E_g^c)	$\lambda_{\text{max}}^{\text{film}^b}$ (nm)	(E_g^c)	$E_{\text{red1}}^{\text{onset}^d}$ (V)	LUMO ^e (eV)
M1	591 (2.0)		617 (1.9)		−0.08	−4.22
M2	523 (2.2)		556 (2.1)		−0.43	−3.86
D1	608 (1.7)		802 (1.4)		−0.03	−4.25
D2	528 (1.9)		666 (1.6)		−0.32	−3.94

^aMaximum end absorption wavelength of the UV–vis spectrum in CH_2Cl_2 . ^bMaximum end absorption wavelength of the UV–vis spectrum in spin-coated thin film on quartz. ^cOptical band gap (E_g) is estimated from the edge of end absorption. ^d Bu_4NPF_6 (0.1 M) in CH_2Cl_2 (vs SCE) using ferrocene as an internal standard at scan rate of 50 mV/s. ^eEstimated from the equation $E(\text{LUMO}) = -(4.8 \text{ eV} - E_{\text{Fc}^+/ \text{Fc}} + E_{\text{red1}}^{\text{onset}})$.

solution, the maximum absorptions of **D1** (608 nm) and **D2** (528 nm) are slightly red-shifted and broadened compared to those of the parent **M1** (591 nm) and **M2** (523 nm), implicating a certain degree of communication between the two adjacent core-expanded NDI subunits in **D1** and **D2**, in spite of the calculated significant intramolecular twist angles. From solution to thin film, the low-energy absorption bands are all red-shifted for **M1**, **M2**, **D1**, and **D2**, suggesting the formation of J-type aggregation in the solid state.¹² The thin film absorptions of **M1** and **M2** express minor bathochromic shifts of 26 and 23 nm relative to their solution patterns, respectively, whereas those of their dimers **D1** and **D2** show much larger bathochromic shifts of 194 and 138 nm, respectively, extending the end absorptions to 802 and 666 nm. Such significant redshifts of **D1** and **D2** may be ascribed to a combined effect of the increased intramolecular conjugation extent and the intermolecular π – π stacking in the solid state. We envision that intermolecular aggregation in the solid state forces the two singly linked core-expanded NDI units of **D1** and **D2** to take a more coplanar conformation. This assumption is further supported by the calculated absorption spectra of **D1** and **D2**, which manifest a very large redshift (130 nm for **D1** and 150 nm for **D2**) from the optimized twisted structure to the corresponding planar conformation (Figure S4). It should be noted that the absorption spectra of both **D1** and **D2** exhibit interesting solvatochromic effects (Figure S3b) where

their long-wavelength absorption bands are both shifted bathochromically when the solvent polarity decreases. The optical band gaps of molecules **M1** and **M2** in solution/thin film are 2.0/1.9 and 2.2/2.1 eV, respectively, estimated from their onset of low-energy absorptions, while **D1** and **D2** have much narrower band gaps of 1.7/1.4 and 1.9/1.6 eV in solution/thin film, respectively, owing to their higher degree of electron delocalization.

The electrochemical properties of the present four compounds (**M1**, **M2**, **D1**, and **D2**) were examined by cyclic voltammetry (CV) in dichloromethane (Figure S5 and Table 1). The reduction processes are observed for these compounds (Figure S5a), and the incorporation of the electron-donating vinylous TTF unit does not lead to detectable oxidative processes for **D1** and **D2** during the CV measurements with the voltage of up to 1.5 V (Figure S5b). The results demonstrate that these vinylous TTFs with the fused NDI moieties (**D1** and **D2**) are more like electron acceptors than donors. The first onset reductive potentials ($E_{\text{red1}}^{\text{onset}}$) are determined at −0.08, −0.43, −0.03, and −0.32 V for **M1**, **M2**, **D1**, and **D2**, respectively. The more positive reduction potentials of **M1** and **D1** versus those of **M2** and **D2** arise from the electron-withdrawing character of the DTYM group.⁷ The LUMO energy levels, estimated from the onset reductive potentials, are positioned at −4.22, −3.86, −4.25, and −3.94 V for **M1**, **M2**, **D1**, and **D2**, respectively.

To study the charge-transport properties of **D1** and **D2**, organic thin film transistors (OTFTs) based on **D1** and **D2** were fabricated by spin coating from their respective *o*-dichlorobenzene (ODCB) or xylene solutions on octadecyltrichlorosilane (OTS)-treated SiO_2/Si substrates, affording a bottom-gate, top-contact device configuration. As shown in Figure 4, all devices

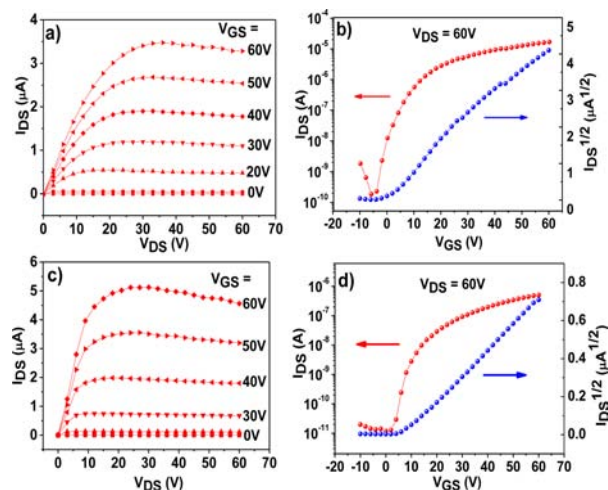


Figure 4. Output and transfer characteristics of OTFT devices based on **D1** (a, b) and **D2** (c, d).

exhibited typical n-channel characteristics under ambient conditions, and the device performance was summarized in Table S1. OTFTs based on **D1** present a stepwise enhancement of electron mobility upon thin-film thermal annealing relative to the as-spun thin-film devices (average mobility $<0.1 \text{ cm}^2 \text{ V}^{-1} \text{ s}^{-1}$). Thin films of **D1** processed from xylene solution exhibited even higher device performance than those processed from ODCB solution with a maximum electron mobility of $0.35 \text{ cm}^2 \text{ V}^{-1} \text{ s}^{-1}$ (average value: $0.31 \text{ cm}^2 \text{ V}^{-1} \text{ s}^{-1}$) and an on/off ratio of 10^6 after annealing at 180°C . The as-spun thin films of **D2** processed from ODCB solution presented high electron

mobilities of up to $0.45 \text{ cm}^2 \text{ V}^{-1} \text{ s}^{-1}$ (average value: $0.34 \text{ cm}^2 \text{ V}^{-1} \text{ s}^{-1}$), which are much higher than those prepared from xylene solution (average mobility: $0.10 \text{ cm}^2 \text{ V}^{-1} \text{ s}^{-1}$), but further thermal annealing on thin films of **D2** did not increase the device performance efficiently. It should be noted that the pure electron-transporting behaviors of these NDI-fused vinyllogous TTFs (**D1** and **D2**) are quite different from the hole-transporting features of the NDI derivatives with two fused TTF units on the central naphthalene core.¹³

XRD results (Figure S6) show distinct diffraction peaks for thin films of **D1** and **D2**, suggesting crystalline films formed on the substrates. AFM images of thin films of **D1** show obvious solvent-dependent morphology: ODCB spin-coated films reveal generally smooth but discontinuous features with evident cracks (Figure 5a), while xylene spin-coated films exhibit a micronano

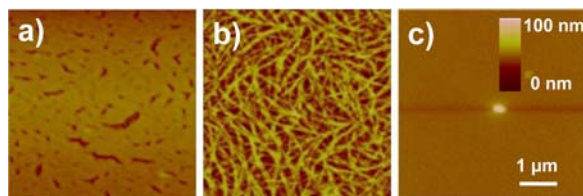


Figure 5. AFM images of the as-spun thin films of **D1** (a, spin-coated from ODCB solution; b, casted from xylene solution) and **D2** (c, spin-coated from ODCB solution) in trapping mode.

fiberlike network structure (Figure 5b) that shows limited morphology changes upon thermal annealing. This fibrous morphology may hint at ordered molecular orientations and strong intermolecular electron coupling between closely packed molecules, which is beneficial for charge transport.¹⁴

In conclusion, the first two examples of electron-transporting vinyllogous TTFs (**D1** and **D2**) were developed by the dimerization of core-expanded NDIs, which both contain a dicyano-substituted vinyllogous TTF unit. These NDI-fused vinyllogous TTFs showed long-wavelength and broadened absorptions of up to the near-infrared absorption region and the reduction (electron-accepting) electrochemical behavior. The solution-processed OTFT devices based on **D1** and **D2** exhibit unipolar n-channel characteristics with electron mobilities of up to $0.45 \text{ cm}^2 \text{ V}^{-1} \text{ s}^{-1}$. The results demonstrate that these NDI-fused vinyllogous TTFs are excellent electron acceptors and bring about new insights into the chemistry of vinyllogous TTFs.

■ ASSOCIATED CONTENT

Supporting Information

The Supporting Information is available free of charge on the ACS Publications website at DOI: 10.1021/acs.orglett.6b03614.

Experimental details, synthetic details, characterization data, TGA, DSC, UV-vis spectra, cyclic voltammetry, XRD, OTFT, as well as calculation data (PDF)

■ AUTHOR INFORMATION

Corresponding Author

* E-mail: gaoxk@mail.sioc.ac.cn

ORCID

Xike Gao: 0000-0003-2740-5529

Notes

The authors declare no competing financial interest.

■ ACKNOWLEDGMENTS

This research was financially supported by the National Natural Science Foundation (20902105 and 21522209), the "Strategic Priority Research Program" (XDB12010100), and the Shanghai Science and Technology Committee (No. 16JC1400603).

■ REFERENCES

- (1) Yoshida, Z.-i.; Kawase, T.; Awaji, H.; Sugimoto, I.; Sugimoto, T.; Yoneda, S. *Tetrahedron Lett.* **1983**, *24*, 3469.
- (2) Misaki, Y.; Higuchi, N.; Fujiwara, H.; Yamabe, T.; Mori, T.; Mori, H.; Tanaka, S. *Angew. Chem., Int. Ed. Engl.* **1995**, *34*, 1222.
- (3) (a) Sugimoto, T.; Awaji, H.; Sugimoto, I.; Misaki, Y.; Kawase, T.; Yoneda, S.; Yoshida, Z.-i.; Kobayashi, T.; Anzai, H. *Chem. Mater.* **1989**, *1*, 535. (b) Bryce, M. R.; Moore, A. J.; Tanner, B. K.; Whitehead, R.; Clegg, W.; Gerson, F.; Lamprecht, A.; Pfenninger, S. *Chem. Mater.* **1996**, *8*, 1182.
- (4) Bellec, N.; Boubekeur, K.; Carlier, R.; Hapiot, P.; Lorcy, D.; Tallec, A. *J. Phys. Chem. A* **2000**, *104*, 9750.
- (5) (a) Jia, C.; Liu, S.-X.; Neels, A.; Stoeckli-Evans, H.; Decurtins, S. *Synthesis* **2005**, 2157. (b) Guerro, M.; Lorcy, D. *Tetrahedron Lett.* **2005**, *46*, 5499.
- (6) (a) Zhao, Y.; Chen, G.; Mulla, K.; Mahmud, I.; Liang, S.; Dongare, P.; Thompson, D. W.; Dawe, L. N.; Bouzan, S. *Pure Appl. Chem.* **2012**, *84*, 1005. (b) Gontier, E.; Bellec, N.; Brignou, P.; Gohier, A.; Guerro, M.; Roisnel, T.; Lorcy, D. *Org. Lett.* **2010**, *12*, 2386. (c) Liang, S.; Zhao, Y.; Adronov, A. *J. Am. Chem. Soc.* **2014**, *136*, 970. (d) Khadem, M.; Walsh, J. C.; Bodwell, G. J.; Zhao, Y. *Org. Lett.* **2016**, *18*, 2403.
- (7) (a) Gao, X.; Di, C.; Hu, Y.; Yang, X.; Fan, H.; Zhang, F.; Liu, Y.; Li, H.; Zhu, D. *J. Am. Chem. Soc.* **2010**, *132*, 3697. (b) Hu, Y.; Gao, X.; Di, C.; Yang, X.; Zhang, F.; Liu, Y.; Li, H.; Zhu, D. *Chem. Mater.* **2011**, *23*, 1204. (c) Hu, Y.; Qin, Y.; Gao, X.; Zhang, F.; Di, C.; Zhao, Z.; Li, H.; Zhu, D. *Org. Lett.* **2012**, *14*, 292. (d) Zhang, F.; Hu, Y.; Schuettfort, T.; Di, C.; Gao, X.; McNeill, C. R.; Thomsen, L.; Mannsfeld, S. C. B.; Yuan, W.; Sirringhaus, H.; Zhu, D. *J. Am. Chem. Soc.* **2013**, *135*, 2338. (e) Hu, Y.; Wang, Z.; Zhang, X.; Yang, X.; Li, H.; Gao, X. *Chin. J. Chem.* **2013**, *31*, 1428. (f) Zhao, Z.; Zhang, F.; Hu, Y.; Wang, Z.; Leng, B.; Di, C.; Zhu, D. *ACS Macro Lett.* **2014**, *3*, 1174. (g) Gao, X.; Hu, Y. *J. Mater. Chem. C* **2014**, *2*, 3099. (h) Leng, B.; Lu, D.; Jia, X.; Yang, X.; Gao, X. *Org. Chem. Front.* **2015**, *2*, 372.
- (8) (a) Gao, X.; Qiu, W.; Yang, X.; Liu, Y.; Wang, Y.; Zhang, H.; Qi, T.; Liu, Y.; Lu, K.; Du, C.; Shuai, Z.; Yu, G.; Zhu, D. *Org. Lett.* **2007**, *9*, 3917. (b) Hu, Y.; Wang, Z.; Yang, X.; Zhao, Z.; Han, W.; Yuan, W.; Li, H.; Gao, X.; Zhu, D. *Tetrahedron Lett.* **2013**, *54*, 2271.
- (9) Polander, L. E.; Romanov, A. S.; Barlow, S.; Hwang, D. K.; Kippelen, B.; Timofeeva, T. V.; Marder, S. R. *Org. Lett.* **2012**, *14*, 918.
- (10) Balandier, J. Y.; Quist, F.; Amato, C.; Bouzakraoui, S.; Cornil, J.; Sergeyev, S.; Geerts, Y. *Tetrahedron* **2010**, *66*, 9560.
- (11) Coropceanu, V.; Cornil, J.; da Silva Filho, D. A.; Olivier, Y.; Silbey, R.; Brédas, J.-L. *Chem. Rev.* **2007**, *107*, 926.
- (12) Jelley, E. E. *Nature* **1936**, *138*, 1009.
- (13) Tan, L.; Guo, Y.; Yang, Y.; Zhang, G.; Zhang, D.; Yu, G.; Xu, W.; Liu, Y. *Chem. Sci.* **2012**, *3*, 2530.
- (14) (a) Wang, S.; Pisula, W.; Müllen, K. *J. Mater. Chem.* **2012**, *22*, 24827. (b) Briseno, A. L.; Mannsfeld, S. C. B.; Shamberger, P. J.; Ohuchi, F. S.; Bao, Z.; Jenekhe, S. A.; Xia, Y. *Chem. Mater.* **2008**, *20*, 4712.